Phase diagrams of the two-orbital Hubbard model with different bandwidths

Kensuke Inaba and Akihisa Koga

Department of Applied Physics, Osaka University, Suita, Osaka 565-0871, Japan

We investigate the two-orbital Hubbard model in infinite dimensions by means of the self-energy functional method. By calculating the entropy, susceptibility, and quasi particle weight at zero temperature, we determine the phase diagram for the system with same and different bandwidths, which is compared with that obtained recently. It is clarified that orbital fluctuations play a key role in controlling the nature of the Mott transitions in the system.

I. INTRODUCTION

Transition metal oxides have attracted much interest in their various aspects.[1,2] Among them, heavy-fermion behavior in d-electron systems stimulates experimental and theoretical investigations. One of typical examples is the lithium vanadate LiV_2O_4,[3] where heavy-fermion behavior with the enhanced specific-heat coefficient $\gamma_e = 0.42$ J/mol K^2 has been observed at low temperatures. It has been suggested that the large mass enhancement in this system may originate from geometrical frustration.[4–6] Recently, it has been pointed out that degenerate orbitals in the t_{2g} subshell also play an important role in realizing heavy-fermion behavior in LiV_2O_4.[7,8] Another example is the isovalent ruthenate arroy $Ca_{2-x}Sr_xRuO_4$. In the compound, the substitution of Ca^{2+} ions for $x > 0.5$ realizes heavy fermions in the t_{2g} subshell,[9] where some of physical quantities have a cusp singularity around $x = 0.5$. Furthermore, the unexpected $s = 1/2$ moment per Ru ion coexisting with the metallic state has been observed in that region,[9] which suggests the existence of the orbital-selective Mott transition (OSMT).[10,11] This type of the Mott transition has also been suggested to occur in the compound $La_{n+1}Ni_nO_{3n+1}$,[12,13] stimulating further experimental investigations of the multiorbital systems.

In the above compounds, electron correlations in the system with orbital degeneracy are important in understanding heavy-fermion behavior. In particular, the concept of the OSMT provides a new paradigm of metal-insulator transitions in multiorbital systems. Although intensive theoretical studies of these topics have recently been done,[10,11,14–49] there are some controversial conclusions even in the simplest multiorbital model. In fact, in the infinite-dimensional two-band system with equivalent orbitals, the existence of Hund coupling induces the first-order Mott transition to the insulating phase.[17,28,44] However, recent results obtained by dynamical mean-field theory[50,51] (DMFT) combined with the numerical renormalization group claim that the Mott transition is of second order in a certain parameter region.[29] In addition, there are some open questions about the system with different bandwidths. It has been pointed out that double OSMTs occur in general, which merge to a single Mott transition only under special conditions.[31–33,35] On the other hand, it has been proposed that double transitions always occur if the system has a large difference of the bandwidths.[38,39] Therefore, it is highly desired to discuss the nature of the Mott

transition in order to clarify what triggers the single or double transitions in the system with different bandwidths.

Motivated by this, we investigate Mott transitions in multiorbital systems. In particular, we focus on orbital fluctuations in this paper, which may play an important role in stabilizing the metallic state in the system.[24,36] By making use of the self-energy functional approach (SFA) proposed by Potthoff,[52,53] we confirm some previous works[38,39] and determine the phase diagrams. We examine how orbital fluctuations are affected by the Hund coupling and/or the difference of the bandwidths to clarify that the enhanced orbital fluctuations make single Mott transitions stable against double OSMTs.

This paper is organized as follows. In Sec. II, we introduce the two-orbital Hubbard model and briefly summarize the SFA.[52,53] The nature of the Mott transitions in the two-orbital system with same bandwidths is discussed in Sec. III. We also discuss how the OSMT is realized in a system with different bandwidths in Sec. IV. A brief summary is given in Sec. V.

II. MODEL AND METHOD

We consider the two-orbital Hubbard model with different bandwidths, which is given by the Hamiltonian $\mathcal{H} = \mathcal{H}_0 + \mathcal{H}'$, $\mathcal{H}' = \Sigma_i \mathcal{H}_i'$ with

$$\mathcal{H}_0 = \sum_{\langle i,j \rangle, \alpha, \sigma} (t_\alpha - \mu \delta_{ij}) c_{i\alpha\sigma}^\dagger c_{j\alpha\sigma}, \qquad (1)$$

$$\mathcal{H}_i' = U \sum_\alpha n_{i\alpha\uparrow} n_{i\alpha\downarrow} + \sum_{\sigma\sigma'} (U' - \delta_{\sigma\sigma'} J) n_{i1\sigma} n_{i2\sigma'}$$

$$- J(c_{i1\uparrow}^\dagger c_{i1\downarrow} c_{i2\downarrow}^\dagger c_{i2\uparrow} + c_{i1\uparrow}^\dagger c_{i1\downarrow} c_{i2\uparrow}^\dagger c_{i2\downarrow} + \mathrm{H.c.}), \quad (2)$$

where $c_{i\alpha\sigma}^\dagger (c_{i\alpha\sigma})$ creates (annihilates) an electron with spin $\sigma (=\uparrow, \downarrow)$ and orbital $\alpha (=1, 2)$ at the i th site and $n_{i\alpha\sigma}$ is the number operator. Here, t_α denotes the hopping integral for the αth orbital, μ the chemical potential, $U (U')$ the intra orbital (inter orbital) Coulomb interaction, and J the Hund coupling including the spin-flip and pair-hopping terms. In the paper, we impose the condition $U = U' + 2J$ due to the rotational symmetry of degenerate orbitals.

To discuss the Mott transitions in the multiorbital systems, we make use of the SFA. Since this method is based on the

variational principle, it has an advantage to discuss the properties of the Mott transition systematically. In fact, it has successfully been applied to various systems such as Hubbard models in infinite dimensions[52–56] and finite dimensions.[57–63]

In this approach, the ground potential Ω is given as

$$\Omega[\Sigma] = F[\Sigma] + \mathrm{Tr} \ln[-(G_0^{-1} - \Sigma)^{-1}], \tag{3}$$

where $F[\Sigma]$ is the Legendre transformation of the Luttinger-Ward potential.[64] G_0 and Σ are the bare Green function and the self-energy, respectively. Here the Dyson equation $G^{-1} = G_0^{-1} - \Sigma$ is obtained under the condition $\partial\Omega[\Sigma]/\partial\Sigma = 0$,[64] where G is the full Green function. We wish to note that the potential $F[\Sigma]$ does not depend on the details of the noninteracting Hamiltonian.[52] This allows us to introduce a reference system with the same interacting term. The Hamiltonian is explicitly given by $\mathcal{H}_{\mathrm{ref}}(\mathbf{t}') = \mathcal{H}_0(\mathbf{t}') + \mathcal{H}'$ with the parameter matrix $\mathbf{t}'$. Then we obtain the grand potential as

$$\Omega[\Sigma(\mathbf{t}')] = \Omega(\mathbf{t}') + \mathrm{Tr} \ln\{-[\omega + \mu - \mathbf{t} - \Sigma(\mathbf{t}')]^{-1}\}$$
$$- \mathrm{Tr} \ln\{-[\omega + \mu - \mathbf{t}' - \Sigma(\mathbf{t}')]^{-1}\}, \tag{4}$$

where $\Omega(\mathbf{t}')$ and $\Sigma(\mathbf{t}')$ are the grand potential and self-energy for the reference system. The condition $\partial\Omega[\Sigma(\mathbf{t}')]/\partial\mathbf{t}' = 0$ gives us an appropriate reference system $\mathcal{H}_{\mathrm{ref}}(\mathbf{t}')$ in the framework of the SFA.

If the SFA is applied to infinite-dimensional correlated electron systems, an Anderson impurity model is one of the most appropriate reference systems, which is given by

$$\mathcal{H}_{\mathrm{ref}} = \sum_i \mathcal{H}_{\mathrm{ref}}^{(i)}, \tag{5}$$

$$\mathcal{H}_{\mathrm{ref}}^{(i)} = \sum_{\alpha\sigma} \varepsilon_{0\alpha}^{(i)} c_{i\alpha\sigma}^{\dagger} c_{i\alpha\sigma} + \sum_{k=1}^{N_b} \sum_{\alpha\sigma} \varepsilon_{k\alpha}^{(i)} a_{k\alpha\sigma}^{(i)\dagger} a_{k\alpha\sigma}^{(i)}$$
$$+ \sum_{k=1}^{N_b} \sum_{\alpha\sigma} V_{k\alpha}^{(i)} (c_{i\alpha\sigma}^{\dagger} a_{k\alpha\sigma}^{(i)} + \mathrm{H.c.}) + \mathcal{H}_i', \tag{6}$$

where $a_{k\alpha\sigma}^{(i)\dagger}$ ($a_{k\alpha\sigma}^{(i)}$) creates (annihilates) an electron with spin σ and orbital α at the $k(=1,2,\ldots,N_b)$th site, which is connected to the ith site in the original lattice. In the limit of $N_b \to \infty$, the condition $\partial\Omega[\Sigma(\mathbf{t}')]/\partial\mathbf{t}' = 0$ reproduces the self-consistent equations of DMFT.[52–54]

The grand potential per site is rewritten as

$$\Omega/L = \Omega_{\mathrm{imp}} - 2\sum_\alpha \sum_m F(\omega_{\alpha m}') - 2\sum_\alpha \sum_{k=1}^{N_b} F(\omega_{k\alpha}^b)$$
$$+ 2\sum_\alpha \sum_m \int_\infty^{-\infty} dz \rho_\alpha(z) F[\omega_{\alpha m}(z)], \tag{7}$$

$$F(x) = -T \ln[1 + \exp(-x/T)], \tag{8}$$

where Ω_{imp} is the grand potential for the reference system. $\omega_{\alpha m}(z)$ ($\omega_{\alpha m}'$) is the pole of Green function G (G') for the original (reference) system, and $\omega_{k\alpha}^b = \varepsilon_{k\alpha} - \mu$. The Green function of the reference system is given as

$$G_\alpha'(\omega) = [\omega + \mu - \varepsilon_{0\alpha} - \Delta_\alpha(\omega) - \Sigma_\alpha(\omega)]^{-1}, \tag{9}$$

$$\Delta_\alpha(\omega) = \sum_{k=1}^{N_b} \frac{V_{k\alpha}^2}{\omega - \omega_{k\alpha}^b}, \tag{10}$$

where $\Sigma_\alpha(\omega)$ is the self-energy for the αth orbital. On the other hand, the full Green function is given as

$$G_\alpha(\omega; z) = [\omega + \mu - z - \Sigma_\alpha(\omega)]^{-1}. \tag{11}$$

Note that the following differential equation is efficient to deduce the poles $\omega_{\alpha m}(z)$ in the Green function:

$$\frac{d\omega_{\alpha m}(z)}{dz} = \left(1 - \frac{\partial\Sigma_\alpha(\omega)}{\partial\omega}\right)^{-1}_{\omega=\omega_{\alpha m}(z)}. \tag{12}$$

By solving these equations, we estimate the grand potential numerically to discuss the effect of electron correlations.

To clarify the nature of Mott transitions, we calculate various physical quantities. In the metallic phase, the quasiparticle weight for the αth orbital, Z_α, is useful to discuss how the Fermi-liquid states are renormalized by the Coulomb interactions. This quantity is proportional to the inverse of the effective mass, which is defined as

$$Z_\alpha^{-1} = \left(1 - \frac{\partial\Sigma_\alpha(\omega)}{\partial\omega}\right)_{\omega=0}. \tag{13}$$

Furthermore, we calculate the local susceptibilities, which may clarify how spin, orbital, and charge fluctuations affect the stability of the metallic state. These read

$$\chi_s = \int_0^\beta \langle \mathcal{T}[n_\uparrow(\tau) - n_\downarrow(\tau)][n_\uparrow(0) - n_\downarrow(0)]\rangle d\tau,$$

$$\chi_o = \int_0^\beta \langle \mathcal{T}[n_1(\tau) - n_2(\tau)][n_1(0) - n_2(0)]\rangle d\tau,$$

$$\chi_c = \int_0^\beta \langle \mathcal{T}[n(\tau) - 2][n(0) - 2]\rangle d\tau, \tag{14}$$

where $n = \sum_{\alpha\sigma} n_{\alpha\sigma}$, $n_{\sigma(\alpha)} = \sum_{\alpha(\sigma)} n_{\alpha\sigma}$ and $n_{\alpha\sigma} = c_{i\alpha\sigma}^{\dagger} c_{i\alpha\sigma}$, $\mathcal{T}$ the time-ordered operator, $A(\tau) = e^{-\mathcal{H}\tau} A e^{\mathcal{H}\tau}$, and β the inverse temperature. Note that in infinite dimensions, these local quantities coincide with those for the reference system with $N_b \to \infty$.[50] In this paper, calculating these quantities approximately in terms of the reference system with a finite N_b, we discuss how fluctuations affect the stability of the metallic state. We also calculate the residual entropy in the system to characterize the Mott insulating phase, where localized electrons are realized with the free spins. It is given as

$$S = -\frac{d\Omega}{dT} \tag{15}$$

$$=S_{imp} + 2\sum_{\alpha}\sum_{m} F'(\omega'_{\alpha m}) + 2\sum_{\alpha}\sum_{k=1}^{N_b} F'(\omega^b_{k\alpha})$$

$$-2\sum_{\alpha}\sum_{m}\int_{\infty}^{-\infty} dz \rho_{\alpha}(z) F'[\omega_{\alpha m}(z)], \qquad (16)$$

$$F'(x) = [F(x) - (x - \partial x/\partial T)f(x)]/T, \qquad (17)$$

$$f(x) = 1/[1 + \exp(x/T)], \qquad (18)$$

where $S_{imp} = -\partial\Omega_{imp}/\partial T$ is the entropy of the reference system and we have used the condition $\partial\Omega/\partial \mathbf{t}' = 0$. Note that the temperature derivative of the poles for the reference system is zero: $\partial\omega'_{\alpha m}/\partial T = 0$. By estimating $\partial\omega_{\alpha m}(z)/\partial T$ carefully,[54] we can calculate the entropy for the system.

Here, we use the semicircular density of states $\rho_{\alpha}(\omega) = 4/\pi W_{\alpha}\sqrt{1 - (2x/W_{\alpha})^2}$, where $W_{\alpha} (=4t_{\alpha})$ is the bandwidth for the αth orbital, which corresponds to an infinite-coordination Bethe lattice. In this paper, we restrict our discussions to the paramagnetic case in the half-filled system by setting the chemical potential $\mu = U/2 + U' - J/2$. In the following, by varying the ratio of the bandwidths $R \equiv W_1/W_2 (<1)$ with a fixed $t_2 = 1$ (that is, an energy unit), we proceed to discuss the Mott transitions in the two-orbital model.

III. MOTT TRANSITION IN THE SYSTEM WITH THE SAME BANDWIDTHS

Let us consider the two-orbital system with the same bandwidths. Mott transitions in the system have been discussed so far by combining DMFT with numerical techniques.[10,11,14–49] An exact diagonalization study claimed that the first-order transition occurs with the jump in physical quantities.[28] In contrast, it was suggested that the second-order transition occurs in a certain parameter region by means of the numerical renormalization group.[29] In this section, to resolve the controversial conclusions for the properties of the Mott transition, we make use of the SFA with $N_b = 1$. At the end of the section, we check the validity of our analysis by comparing the results of $N_b = 1$ with those of $N_b = 3$.

We first calculate the ground potential Ω as a function of $V \equiv V_{1,1} = V_{1,2}$ at zero temperature, as shown in Fig. 1.

When U is small, it is found that the grand potential has a minimum at finite V. The hybridization V in the reference system, roughly speaking, represents the effective bandwidth for the original system. Therefore, the metallic state is stabilized in this case. It is seen that the increase of the Coulomb interaction with a fixed ratio $J/U = 0$ shifts the stationary point toward the origin continuously. This implies that the effective bandwidth is gradually decreased and the transition occurs to the Mott insulating phase at $U = U_c$. In contrast, the introduction of the Hund coupling leads to different behavior. For instance, we focus on the system with the weak Hund coupling $J/U = 0.03$. When $U = 5$, a minimum appears at $V \sim 0.58$, where the metallic ground state is realized. The increase of the Coulomb interaction induces another mini-
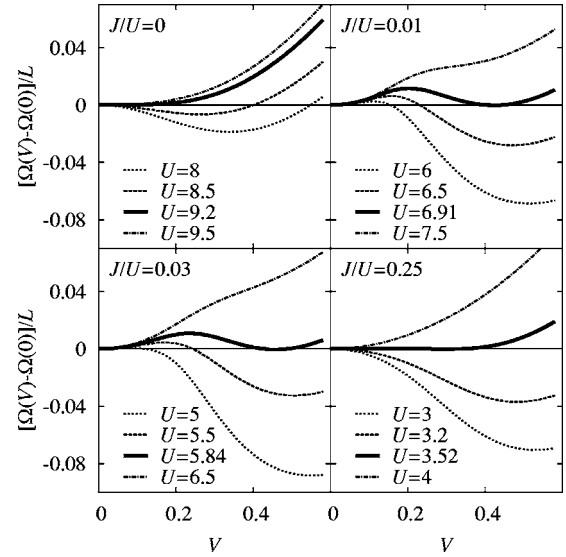

FIG. 1. The grand potential as a function of the variational parameter V. Thick lines correspond to the critical value U_c.

mum around $V \sim 0$, which represents the insulating state. This double-well structure in the grand potential suggests the existence of a first-order Mott transition in the system. By comparing the energy for each state, we determine the critical value $U_c = 5.84$. A similar structure is also observed in the case $J/U = 0.25$. However, the potential barrier between these two states becomes small at a first-order transition point, as shown in Fig. 1. Therefore, it is expected that the singularity characteristic of the first-order transition is more difficult to be observed in this case.

These features mentioned above can be seen in the physical quantities. Here, we show the entropy per site S/L in Fig. 2. $J/U = 0$, the increase of the Coulomb interaction triggers the Mott transition at $U = U_c$, where the entropy jumps up to $S/L = \ln 6$. The value is explained by the fact that sixth-degenerate states are lowest in the atomic limit. On the other hand, the Hund coupling forms triply degenerate states in the limit. Therefore, when $J/U \neq 0$, $S/L = \ln 3$ appears in the insulating phase. It is found that the second-order transition occurs in the system $J/U = 0$, while the first-order transition with the hysteresis occurs in the system with the Hund coupling. For example, when $J/U = 0.03$, the metallic state is
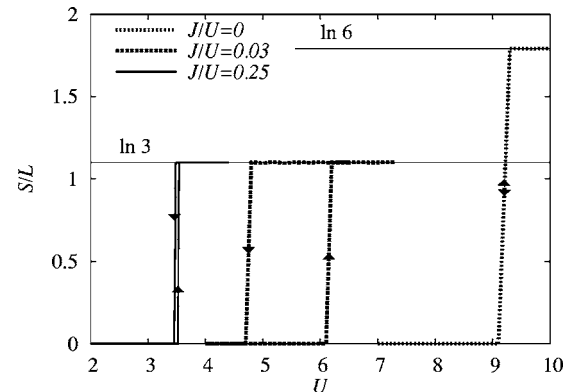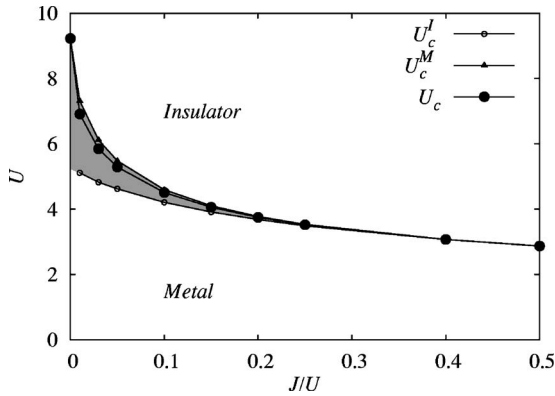

FIG. 2. The entropy per site as a function of U.

FIG. 3. The zero-temperature phase diagram for the degenerate Hubbard model with same bandwidths $R=1$. U_c^I (U_c^M) is the critical point where the insulating (metallic) state disappears. U_c represents the first-order transition points and the shaded region represents the coexisting state.
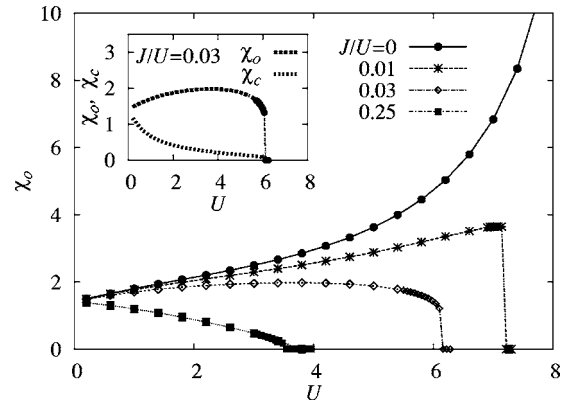

FIG. 4. The local orbital susceptibility in the system with same bandwidths. The inset shows orbital and charge susceptibilities in the case $J=0.03U$.

stabilized up to the critical point $U_c^M=6.12$, while the insulating state is stabilized down to the critical point $U_c^I=4.82$. Note that these critical points U_c^M and U_c^I induced by the Hund coupling at zero temperature are different from critical points U_{c1} and U_{c2}, which are defined as Mott critical points at finite temperatures. Therefore, an inequality $U_c^I \leqslant U_c^M$ is not necessarily satisfied, which will be discussed in detail in the next section.

By performing similar calculations, we obtain the phase diagram as shown in Fig. 3. We find that the phase boundary U_c^M is always larger than U_c^I except for the special condition $J/U=0$. This implies that the first-order Mott transition, in general, occurs in the two-orbital system with the same bandwidths. When the system has the special condition $J/U=0$, the critical point U_c^I ($=U_c^M=9.24$) is different from the extrapolation of the curve U_c^I.[44] This exception may originate from the discontinuity of the residual entropy for the Mott insulating phase. It is also found that the coexisting region bounded by these two lines shrinks with an increase of the Hund coupling J. This interesting feature may be due to orbital fluctuations, which sometimes play an important role in understanding the Mott transitions in the two-orbital system.

To make this point clear, we also calculate the local orbital susceptibility in the metallic state ($U<U_c^M$), as shown in Fig. 4. When $J/U=0$, the increase of the Coulomb interaction enhances the spin and orbital susceptibilities (the spin susceptibility is not shown). Eventually, these quantities diverge simultaneously at the transition point. On the other hand, when one turns on the Hund coupling ($J/U=0.01$), different behavior appears. The introduction of the Coulomb interaction first enhances orbital fluctuations by reflecting the high symmetry $U \sim U'$. Further increase of the interactions renormalizes electrons in both orbitals, where the Hund coupling has a tendency to suppress orbital fluctuations. In fact, in contrast to the case $U=U'$, the orbital susceptibility is much smaller around the Mott critical point. We also find a sudden decrease of the orbital susceptibility where the first-order Mott transition occurs. When the system is located far from the condition $U=U'$, the increase of the Coulomb in-

teraction suppresses orbital fluctuations strongly. Therefore, a tiny jump appears in the curve at $U_c^M=3.54$ ($J/U=0.25$).

The results obtained may shed light on the nature of the Mott transitions in the two-orbital systems with same bandwidths. When $J/U=0$, the second-order Mott transition occurs to the insulating phase. On the other hand, the introduction of the Hund coupling induces the first-order transition with the hysteresis in the physical quantities. It is also found that as J is increased, orbital fluctuations are suppressed strongly, where the singularity for the transition becomes obscure. In this case, the system can be regarded as the system with independent orbitals. Therefore, the OSMT is expected to occur if the bandwidths are different from each other, which will be discussed in the next section. We wish to comment on related recent work.[28,29] The introduction of Hund coupling is known to induce a first-order transition, while the nature of transitions in the large-J region has not been clarified up to now. In the region, the first- (second-) order transition was suggested by the exact diagonalization (numerical renormalization group). On the other hand, our systematic analysis shows a jump singularity in the curve for each physical quantity, except for the $J=0$ case. Therefore, we believe that a further increase of the Hund coupling does not induce a second-order Mott transition in the system with the same bandwidths.

Before closing this section, we would like to check the validity of our analysis. In Fig. 5, we show the quasiparticle weights obtained by the SFA with $N_b=1$ and $N_b=3$. If the Coulomb interactions are introduced, the quasiparticle weight is decreased from unity. In this region, it is found that the quasi particle weight obtained for the system $N_b=1$ is slightly larger than that for the system $N_b=3$. On the other hand, when the system approaches the Mott transition point, the quasiparticle weight is hardly affected by the number of the sites for the reference system. This result may be explained by the fact that the simplified reference system ($N_b=1$) can describe the low-energy physics around the Fermi level and thereby we can determine the critical point quantitatively.[52–54] However, the reference system $N_b=1$ does not describe the high-energy part properly, resulting in an overestimate of Z in the intermediate region.

Similar behavior is also observed in the finite-J case, as shown in Fig. 6. As the Hund coupling is increased, the
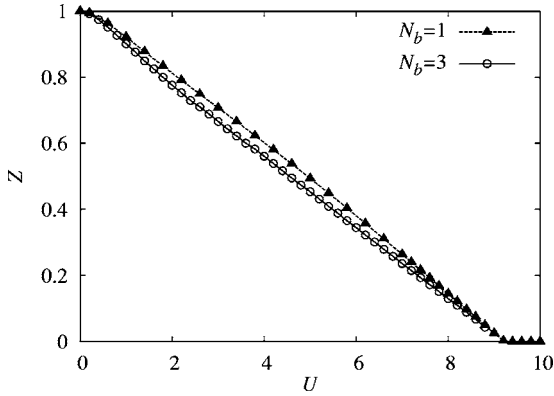
FIG. 5. The quasiparticle weight Z as a function of U obtained from the reference systems $N_b=1$ and $N_b=3$ when $J/U=0$.

Fermi-liquid state is stabilized up to $U_c^M \sim 7.3$ and 3.5 at $J/U=0.01$ and 0.25, respectively, where the first-order transition occurs. It is found that the jump singularity for $N_b=3$ is weaker than that for $N_b=1$, which may cause one to expect that the transition becomes of second order in the $N_b \to \infty$ case. According to the results for the single-band model,[52–54] however, the physical quantities for $N_b=3$ nearly equal those for $N_b>3$. Therefore, we believe that the nature of the Mott transition is hardly affected by N_b and the first-order transition remains in the $N_b \to \infty$ case. In addition, we also find that the critical point U_c^M weakly depends on the number of sites, N_b, implying that the obtained phase boundaries shown in Fig. 3 have been determined rather well even by the reference system $N_b=1$.

IV. ORBITAL-SELECTIVE MOTT TRANSITIONS vs SINGLE MOTT TRANSITION

In this section, we consider Mott transitions in the two-orbital system with different bandwidths ($R \neq 1$).[10,11,31–43,45–49] It has been suggested that in the system with $R=0.5$, the OSMT occurs in the case $J/U=0.25$, while a single Mott transition occurs in the case $J/U=0.[32,35]$ On the other hand, it was recently claimed that double transitions always occur in the small-R case.[38,39] By means of the
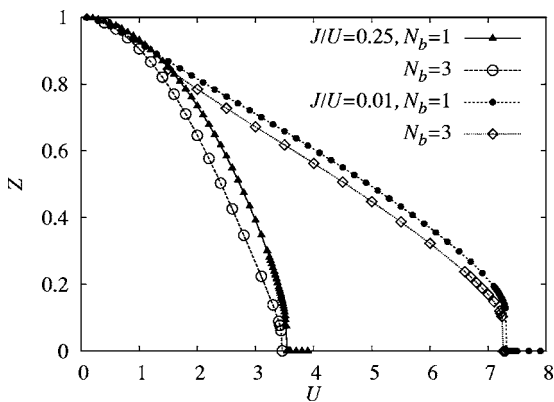

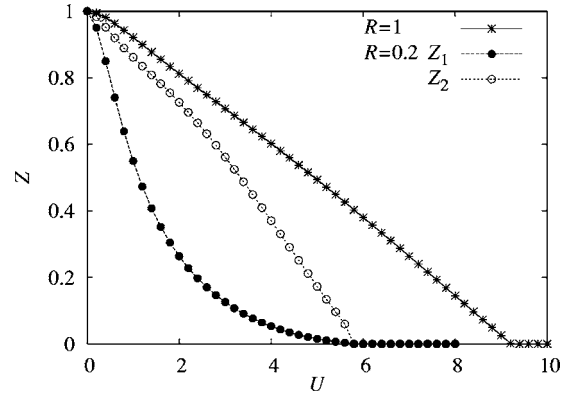FIG. 6. The quasiparticle weight Z as a function of U in the cases $J/U=0.01$ and $J/U=0.25$.

SFA with $N_b=1$, we determine a detailed phase diagram to discuss the nature of the Mott transitions systematically.

First we consider the system without Hund coupling ($J/U=0$). In the system with the same bandwidths ($R=1$), a second-order Mott transition occurs at $U_c=9.24$, where the quasiparticle weight continuously reaches zero and the orbital susceptibility diverges. Away from the condition (e.g., $R=0.2$), the introduction of the interaction decreases the quasiparticle weights Z_1 and Z_2 in different ways, reflecting the difference of bandwidths, as shown in Fig. 7. This enhances the spin fluctuations and suppresses orbital fluctuations. However, when the system approaches the Mott transition point, the effect of the bare bandwidths is diminished due to the strong renormalization, which enhances both spin and orbital fluctuations. Therefore, in the case $R=0.2$, monotonic (nonmonotonic) behavior appears in the curves of the spin (orbital) susceptibility. As a consequence, a single Mott transition occurs, where the quasi particle weight for each orbital vanishes simultaneously.[35] On the other hand, somewhat different behavior appears in the case $R<R_c(=0.192)$, as shown in the inset of Fig. 8. If the Coulomb interactions are increased, orbital fluctuations are strongly suppressed due to the difference of the effective Coulomb interactions. In this case, the orbital susceptibility never diverges, which suggests the existence of the OSMT, as discussed by de' Medici *et al.*[39] and Ferrero *et al.*[38] In fact, the OSMT yields a localized

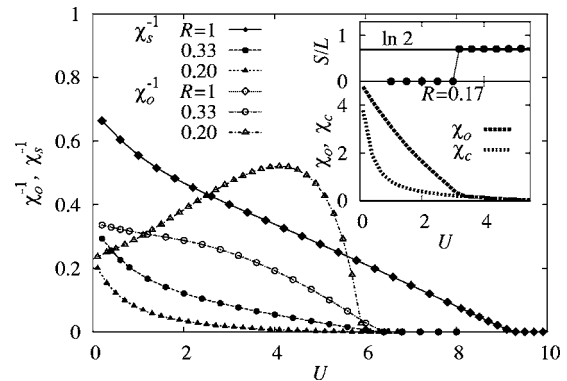FIG. 7. The quasiparticle weights for the αth orbital Z_α when $R=1$ and 0.2.

FIG. 8. The inverse of orbital and spin local susceptibilities as a function of U when $J/U=0$. The inset shows orbital and charge susceptibilities and the entropy per site when $R=0.17$.
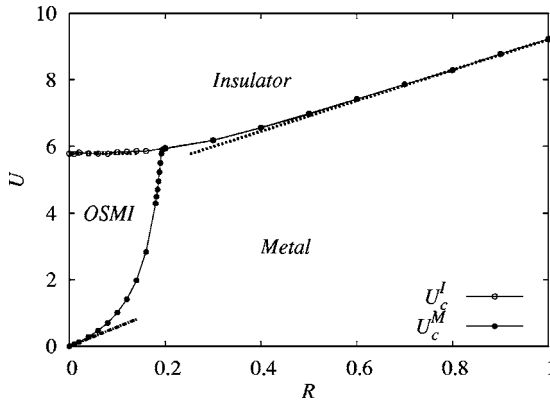
FIG. 9. The phase diagram for the case $J/U=0$. U_c^I (U_c^M) is the critical point where the insulating (metallic) state becomes unstable with increasing (decreasing) U. The dotted lines denote the phase boundaries obtained by a simple estimation (see text).

spin $s=1/2$ at each site. Therefore, the residual entropy $S/L=\ln 2$ appears and the orbital susceptibility merges to the charge susceptibility at $U_c^M \sim 3.2$, as shown in the inset of Fig. 8. Further increase of the Coulomb interaction decreases the charge and orbital susceptibilities and another Mott transition occurs at $U_c^I \sim 5.9$.

By estimating the critical points systematically, we obtain the phase diagram shown in Fig. 9. When $R=1$, the model is reduced to the system with same bandwidths, where the Mott transition occurs between the metallic and Mott insulating phases. Even when the system has two distinct orbitals, a single Mott transition still occurs ($U_c^M=U_c^I$) owing to enhanced orbital fluctuations within the region ($R_c<R<1$). In this region, the phase boundary is simply deduced by the Gutzwiller approximation as $U_c \propto \int d\epsilon \epsilon \rho(\epsilon) = (1+R)/2$, which is in good agreement with the results obtained by the SFA. On the other hand, in the region $R \lesssim R^c$, double Mott transitions occur ($U_c^M < U_c^I$) when the interaction is varied. Then the orbital-selective Mott insulating (OSMI) phase appears between the metallic and insulating phases.[38,39] In the case, the system may be regarded as two independent single-band systems. In fact, the phase boundaries $U_c^I \sim u_c R$ and $U_c^M \sim u_c$, where $u_c=5.85$ is the critical point for the single-band model,[50,53] are in good agreement with our SFA results in the case $R \ll 1$, as shown in Fig. 9. The phase diagram is consistent with that obtained by de' Medici et al.[39] and Ferrero et al.[38]

Next, we consider the effect of Hund coupling in the system with different bandwidths $R=0.5$. In Fig. 10, we show the physical quantities as a function of U with a fixed ratio J/U. When the Hund coupling is small $J/U=0.01$, the interaction renormalizes electrons depending on each bandwidth and it triggers the first-order single transition to the Mott insulating phase at $U_c^M=5.47$. Then, the singularity appears in the curve of the susceptibility and entropy. This implies that the existence of Hund coupling induces a first-order Mott transition with the hysteresis, where the Mott insulating phase is stabilized down to $U_c^I=4.72$. Although this result is the same as that in the system with $R=1$, it does not necessarily imply that the difference of the bandwidths is irrelevant in the whole parameter space. Indeed, further increase
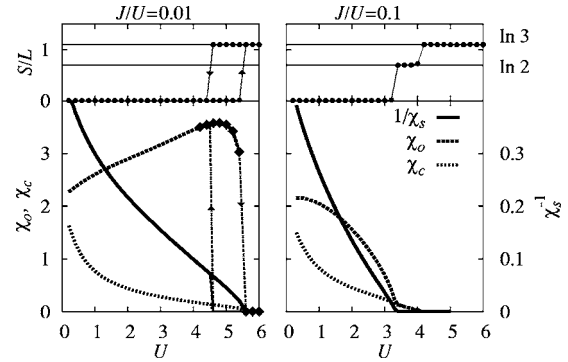

FIG. 10. The local susceptibilities and the entropy per site in the system with different bandwidths $R=0.5$.

of the Hund coupling suppresses orbital fluctuations, leading to double transitions in the system. When $J/U=0.1$, the introduction of the Coulomb interaction decreases the orbital and charge susceptibilities. Consequently, these quantities merge with each other and the spin susceptibility diverges at the critical point $U_c^M=3.34$. This means that the second-order OSMT occurs in the narrower band. Thus, free spins $s=1/2$ are induced at each site, yielding the residual entropy $S/L=\ln 2$. Furthermore, as the interactions are increased, both orbital and charge susceptibilities reach zero at $U_c^I=4.06$.

Performing similar calculations with several choices of R, we end up with the phase diagrams shown in Fig. 11. An important point is that the phase boundaries U_c^M and U_c^I cross each other at $R=R_c$, where $R_c=0.30$ and 0.82 for $J/U=0.1$ and 0.01, respectively. When $R<R_c$, the difference of the bare bandwidths is essential to stabilize the OSMI phase between two phase boundaries ($U_c^M<U<U_c^I$). However, when $R>R_c$, the metallic phase and the Mott insulating phase coexist in the region $U_c^I<U<U_c^M$. In this case, the nature of Mott transitions is similar to that in the system with same bandwidths, where the first-order Mott transition occurs. The above result may suggest that the existence of the OSMT is associated with the first-order transition in the multiorbital Hubbard model with same bandwidths.

To discuss how the coexisting phase competes with the OSMI phase, we also show the phase diagrams with a fixed R in Fig. 12. When $R<0.192$, there always appears an OSMI phase due to the large difference of bandwidths. Note that the
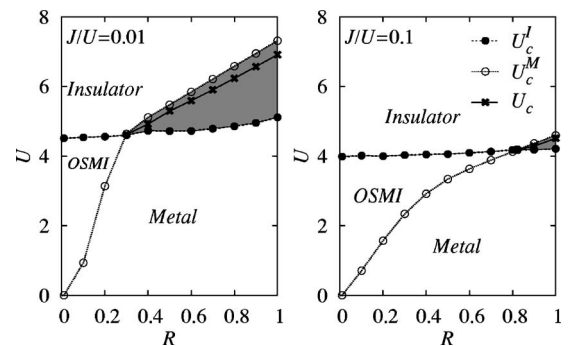

FIG. 11. The phase diagram when $J/U=0.01$ and $J/U=0.1$. The gray region denotes the coexisting state.
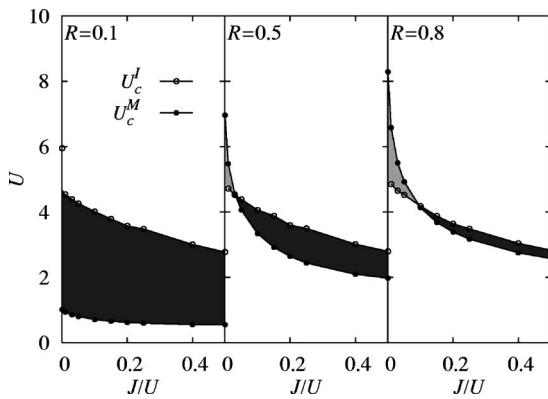
FIG. 12. The phase diagram for the degenerate Hubbard model with different bandwidths $R=0.1$, 0.5 and 0.8. The black and gray regions denote the OSMI phase and the coexisting state, respectively.

phase boundary sometimes has a discontinuity at $J/U=0$, which may originate from the spin and orbital degeneracy of the Mott insulating ground state, as discussed in the previous section. In contrast, the OSMI phase and the coexisting region appear in the case $0.192 < R < 1$. When the system has large Hund coupling, orbital fluctuations are suppressed and the OSMI phase is stabilized. The decrease of J enhances orbital fluctuations in the metallic phase, making the OSMI phase unstable. The phase boundaries then merge at the critical point. Further decrease of the Hund coupling induces a first-order single Mott transition due to enhanced orbital fluctuations, where the coexisting phase appears instead of the OSMI phase. When $R \to 1$, the difference of the bandwidths becomes irrelevant. Therefore, the region of the OSMI phase shrinks and the coexisting phase becomes stable.

Up to now, there were some controversial conclusions for the nature of the OSMT. Most of studies claimed that the second-order OSMT occurs in general.[35,45] In contrast, de' Medici *et al.*[39] and Arita and Held[40] recently claimed that the OSMT is of first order by combining DMFT with the exact diagonalization and the projective quantum Monte Carlo simulations. In our paper, we have calculated the grand po-

tential in the system carefully to clarify that the OSMT is of second order. Although the accuracy of our calculations depends on the size of the reference system in the framework of the SFA, the nature of the Mott transition is hardly affected by the size, as discussed before. Therefore, we believe that the obtained results may shed light on the nature of the Mott transitions in the two-orbital systems.

V. SUMMARY

We have investigated the two-orbital Hubbard model in infinite dimensions to discuss the nature of Mott transitions at half-filling. By making use of the self-energy functional approach, we have clarified that the introduction of Hund coupling induces a first-order transition in the system with the same bandwidths. It has also been found that the increase of the Hund coupling suppresses orbital fluctuations, where the singularity characteristic of the first-order transition becomes obscure. Namely, the upper and lower critical points for the transition approach each other closely, where the weak first-order transition occurs. This behavior is also affected by the difference of the bandwidths. In fact, the difference of the bandwidths suppresses orbital fluctuations, making the first-order transition unstable. As a consequence, the double second-order transitions occur, where the OSMI phase appears between the metallic and Mott insulating phases. Our obtained results reproduce some previous works on the system with same and different bandwidths.[28,29,38,39] Furthermore, taking into account orbital fluctuations carefully, we have resolved some controversial conclusions for the nature of Mott transitions at half-filling.

ACKNOWLEDGMENTS

[1] M. Imada, A. Fujimori, and Y. Tokura, Rev. Mod. Phys. **70**, 1039 (1998).

[2] Y. Tokura and N. Nagaosa, Science **288**, 462 (2000).

[3] S. Kondo *et al.*, Phys. Rev. Lett. **78**, 3729 (1997).

[4] H. Kaps, N. Büttgen, W. Trinkl, A. Loidl, M. Klemm, and S. Horn, J. Phys.: Condens. Matter **13**, 8497 (2001).

[5] M. Isoda and S. Mori, J. Phys. Soc. Jpn. **69**, 1509 (2000).

[6] S. Fujimoto, Phys. Rev. B **64**, 085102 (2001).

[7] H. Tsunetsugu, J. Phys. Soc. Jpn. **71**, 1844 (2002).

[8] Y. Yamashita and K. Ueda, Phys. Rev. B **67**, 195107 (2003).

[9] S. Nakatsuji, D. Hall, L. Balicas, Z. Fisk, K. Sugahana, M. Yoshioka, and Y. Maeno, Phys. Rev. Lett. **90**, 137202 (2003); S. Nakatsuji and Y. Maeno, *ibid.* **84**, 2666 (2000).

[10] V. I. Anisimov, I. A. Nekrasov, D. E. Kondakov, T. M. Rice, and M. Sigrist, Eur. Phys. J. B **25**, 191 (2002).

[11] Z. Fang, N. Nagaosa, and K. Terakura, Phys. Rev. B **69**, 045116 (2004).

[12] K. Sreedhar *et al.*, J. Solid State Chem. **110**, 208 (1994); Z. Zhang *et al.*, *ibid.* **108**, 402 (1994); **117**, 236 (1995).

[13] Y. Kobayashi, S. Taniguchi, M. Kasai, M. Sato, T. Nishioka, and M. Kontani, J. Phys. Soc. Jpn. **65**, 3978 (1996).

[14] C.-I. Kim, Y. Kuramoto, and T. Kasuya, J. Phys. Soc. Jpn. **59**, 2414 (1990).

[15] G. Kotliar and H. Kajueter, Phys. Rev. B **54**, R14221 (1996).

[16] M. J. Rozenberg, Phys. Rev. B **55**, R4855 (1997).

[17] J. Bünemann and W. Weber, Phys. Rev. B **55**, 4011 (1997); J.

Bünemann, W. Weber, and F. Gebhard, *ibid.* **57**, 6896 (1998).

[18] H. Hasegawa, J. Phys. Soc. Jpn. **66**, 3522 (1997).

[19] K. Held and D. Vollhardt, Eur. Phys. J. B **5**, 473 (1998).

[20] J. E. Han, M. Jarrell, and D. L. Cox, Phys. Rev. B **58**, R4199 (1998).

[21] T. Momoi and K. Kubo, Phys. Rev. B **58**, R567 (1998).

[22] A. Klejnberg and J. Spalek, Phys. Rev. B **57**, 12041 (1998).

[23] Y. Imai and N. Kawakami, J. Phys. Soc. Jpn. **70**, 2365 (2001).

[24] A. Koga, Y. Imai, and N. Kawakami, Phys. Rev. B **66**, 165107 (2002); J. Phys. Soc. Jpn. **72**, 1306 (2003).

[25] S. Florens, A. Georges, G. Kotliar, and O. Parcollet, Phys. Rev. B **66**, 205102 (2002).

[26] S. Florens and A. Georges, Phys. Rev. B **66**, 165111 (2002).

[27] V. S. Oudovenko and G. Kotliar, Phys. Rev. B **65**, 075102 (2002).

[28] Y. Ono, M. Potthoff, and R. Bulla, Phys. Rev. B **67**, 035119 (2003).

[29] T. Pruschke and R. Bulla, Eur. Phys. J. B **44**, 217 (2005).

[30] S. Sakai, R. Arita, and H. Aoki, Phys. Rev. B **70**, 172504 (2004).

[31] A. Liebsch, Europhys. Lett. **63**, 97 (2003).

[32] A. Liebsch, Phys. Rev. Lett. **91**, 226401 (2003).

[33] A. Liebsch, Phys. Rev. B **70**, 165103 (2004).

[34] M. Sigrist and M. Troyer, Eur. Phys. J. B **39**, 207 (2004).

[35] A. Koga, N. Kawakami, T. M. Rice, and M. Sigrist, Phys. Rev. Lett. **92**, 216402 (2004).

[36] A. Koga, N. Kawakami, T. M. Rice, and M. Sigrist, Phys. Rev. B **72**, 045128 (2005).

[37] A. Koga, N. Kawakami, T. M. Rice, and M. Sigrist, Physica B **359-361**, 738 (2005).

[38] M. Ferrero, F. Becca, M. Fabrizio, and M. Capone, Phys. Rev. B **72**, 205126 (2005).

[39] L. de' Medici, A. Georges, and S. Biermann, Phys. Rev. B **72**, 205124 (2005).

[40] R. Arita and K. Held, Phys. Rev. B **72**, 201102(R) (2005).

[41] C. Knecht, N. Blümer, and P. G. J. van Dongen, Phys. Rev. B **72**, 081103(R) (2005).

[42] A. Liebsch, Phys. Rev. Lett. **95**, 116402 (2005).

[43] S. Biermann, L. de' Medici, and A. Georges, Phys. Rev. Lett. **95**, 206401 (2005).

[44] K. Inaba, A. Koga, S.-I Suga, and N. Kawakami, Phys. Rev. B **72**, 085112 (2005).

[45] K. Inaba, A. Koga, S. Suga, and N. Kawakami, J. Phys. Soc. Jpn. **74**, 2393 (2005).

[46] A. Ruëgg, M. Indergand, S. Pilgram, and M. Sigrist, Eur. Phys. J. B **48**, 55 (2005).

[47] Y. Song and L. J. Zou, Phys. Rev. B **72**, 085114 (2005).

[48] Y. Tomio and T. Ogawa, J. Lumin. **112**, 220 (2005).

[49] A. Koga, K. Inaba, and N. Kawakami, Prog. Theor. Phys. Suppl. **160**, 253 (2005).

[50] A. Georges, G. Kotliar, W. Krauth, and M. J. Rozenberg, Rev. Mod. Phys. **68**, 13 (1996).

[51] G. Kotliar and D. Vollhardt, Phys. Today **57**(3), 53 (2004).

[52] M. Potthoff, Eur. Phys. J. B **32**, 429 (2003).

[53] M. Potthoff, Eur. Phys. J. B **36**, 335 (2003).

[54] K. Pozgãjčić, cond-mat/0407172 (unpublished).

[55] M. Balzer and M. Potthoff, Physica B **359-361**, 768 (2005).

[56] W. Koller, D. Meyer, A. C. Hewson, and Y. Ono, Physica B **359-361**, 795 (2005).

[57] M. Potthoff, M. Aichhorn, and C. Dahnken, Phys. Rev. Lett. **91**, 206402 (2003).

[58] M. Aichhorn, H. G. Evertz, W. von der Linden, and M. Potthoff, Phys. Rev. B **70**, 235107 (2004).

[59] C. Dahnken, M. Aichhorn, W. Hanke, E. Arrigoni, and M. Potthoff, Phys. Rev. B **70**, 245110 (2004).

[60] N. H. Tong, Phys. Rev. B **72**, 115104 (2005).

[61] D. Senechal, P.-L. Lavertu, M.-A. Marois, and A.-M. S. Tremblay, Phys. Rev. Lett. **94**, 156404 (2005).

[62] M. Aichhorn, E. Y. Sherman, and H. G. Evertz, Phys. Rev. B **72**, 155110 (2005).

[63] M. Aichhorn and E. Arrigoni, Europhys. Lett. **72**, 117 (2005).

[64] J. M. Luttinger, Phys. Rev. **118**, 1417 (1960).